PCCP

Structure of pure SDS and DTAB micelles in brine determined by small-angle neutron scattering (SANS)

Magnus Bergström*† and Jan Skov Pedersen

Condensed Matter Physics and Chemistry Department, Risø National Laboratory, DK-4000 Roskilde, Denmark

Received 30th April 1999, Accepted 5th July 1999

The geometrical structure of pure SDS and DTAB surfactant micelles in the absence of added salt as well as its dependence on the concentration of NaBr have been investigated at 40 °C using small-angle neutron scattering (SANS). In contrast to previous SANS measurements on the same systems we have analysed the scattering data in the entire regime of scattering vectors that are relevant for determining the structure of the micelles. Our obtained results for pure surfactant micelles, as well as those of mixed catanionic micelles presented in a recent study, show somewhat unexpectedly that ordinary surfactant micelles are shaped as circular or elongated bilayers (tablets). Both SDS and DTAB micelles appeared to be disk-like in pure D_2O and the corresponding data were best fitted with a model for (monodisperse) oblate ellipsoids of revolution with half axes $a = 12.0$ Å, $b = 20.3$ Å ([SDS] = 1.0 wt.%) and $a = 12.4$ Å, $b = 21.6$ Å ([DTAB] = 1.0 wt.%). The half axis b related to the disk radius increases in both cases with an increasing amount of added salt to about 23 Å (SDS) and 24 Å (DTAB) at [NaBr] = 0.1 M and at about [NaBr] = 0.2 M the SDS micelles become tablet-shaped, *i.e.* tri-axial ellipsoids with half axes $a < b < c$. For DTAB micelles the disk-to-tablet transition occurs between [NaBr] = 0.5 and 0.7 M. As the amount of salt is further increased the micelles grow strongly with respect to length, but decrease slightly in width to about $b = 20$ Å (SDS) and $b = 22$ Å (DTAB) at [NaBr] = 1.0 M. Half the thickness of the micelles varies only slightly with the solution state and is found to be about 75–90% of the fully extended hydrocarbon chain (= 16.7 Å). Hence, all elongated micelles appeared to have an elliptical cross section with an axial ratio $1.5 < b/a < 1.6$. At [NaBr] = 0.7 M the SDS micelles are considerably elongated and polydisperse and their (volume-weighted) average length increases rapidly with surfactant concentration from about 200 Å at [SDS] = 0.25 wt.% to about 400 Å at [SDS] = 1.0 wt.%. At [NaBr] = 1.0 M the SDS micelles were seen to be shaped as long flexible ribbons too long, *i.e.* several thousands of Angstroms, for their size distribution to be determined from our SANS data whereas DTAB micelles still were rather short, *i.e.* $c = 30$ Å.

Introduction

In pure water ionic surfactants such as sodium dodecyl sulphate (SDS, anionic surfactant) or dodecyltrimethylammonium bromide (DTAB, cationic surfactant) form small (1–2 nm) liquid-like droplets, so called micelles, above a certain concentration. The driving force for the self-assembling of surfactant molecules into micelles is the gain in free energy which is caused by the reduction of the hydrocarbon/water contact area.[1] In order to minimise the hydrocarbon/water contact area per aggregated surfactant this contribution favours a low curvature of the aggregates. Outside the micelle surface, where the head-groups are located, there is a diffuse layer of counter-ions attached to the charged surface, for which the entropy of mixing with solvent increases with the curvature of the aggregate as the counter-ions are spread out in the surrounding bulk solution. In addition, the entropy of mixing surfactant and solvent favours a low number of monomers in each aggregate. As a result, the pure micelles are rather small, *i.e.* their interfaces are rather curved, at low surfactant concentrations in the absence of added salt. The third major free energy contribution to the formation of surfactant micelles is due to the entropy caused by the various chain conformations that are accessible to a surfactant tail enclosed in the hydrophobic core of a micelle.[2–4] This contribution is about ten times smaller in magnitude than the other two but is important so as to yield a minimum in the free energy as a function of the radial thickness for spherical,[5] cylindrical[6] and planar[7] geometry.

In refs. 5–7 the comparatively high macroscopic value of 50 mJ m^{-2} for the hydrocarbon/water interfacial tension was successfully employed in the calculations indicating that the degree of water that penetrates into the hydrocarbon cores is low and, hence, that the hydrocarbon/water interface of the micelles is rather well defined. This is not a surprising result considering the fact that the hydrophobic effect is the driving force for the aggregation process of surfactants in an aqueous solvent.

As an external electrolyte is added to the solutions and mixed into the diffuse layer of counter-ions associated with the micelles, the magnitude of the electrostatic contribution to the free energy is reduced. Moreover, because of geometrical packing constraints the micelles must become increasingly non-spherical as they grow in size. As a result, the growth of rather small micelles into large elongated aggregates with increasing concentration of added salt has been observed using either quasi-elastic light scattering[8] or various nuclear magnetic resonance (NMR) techniques.[9,10] These methods

† Present address: Institute for Surface Chemistry, Box 5607, SE-114 86 Stockholm, Sweden, Tel: + 46 8 790 99 41, Fax: + 46 8 20 89 98, E-mail: magnus.bergstrom@surfchem.kth.se.

are, however, rather insensitive to the detailed geometrical structure of the surfactant aggregates.

The early small-angle neutron scattering (SANS) studies of micelles formed from ionic surfactants mainly concentrated in the large intermicellar double-layer force interactions.[11–15] SANS data with a scattering vector q below about 0.2 Å^{-1} from samples containing SDS and DTAB micelles in the absence of added salt were fitted with conventional models (monodisperse spheres or prolates) of the form factor but the agreements with data for different structures were not compared. Benedouch *et al.*[16] concluded from the scattering behaviour in the range 0.02 Å^{-1} < q < 0.24 Å^{-1} that LDS (dodecyl sulfate, lithium salt) micelles in the absence of added salt are rather polydisperse spheres (12% with respect to the micelle radius). The structure of micelles formed in a 2 wt.% SDS solution at 25 °C was studied with SANS by Cabane *et al.*[17] From the scattering behaviour in the regime of high scattering vectors (q > 0.1 Å^{-1}) they concluded that the micelles are spherically shaped with a comparatively large relative standard deviation $\sigma_R/R = 0.1$ for the number-weighted size distribution. A model fit of the data at both high and low q values was, however, not performed in either ref. 16 or 17. When SANS data (0.02 Å^{-1} < q < 0.24 Å^{-1}) from samples containing pure SDS or TMDS (TM = tetramethylammonium) micelles were investigated with a model for monodisperse spheres with a concentric outer shell of thickness ~ 11 Å, consisting of approximately four methylene groups per surfactant, head-groups, co- and counter-ions in water (Stern layer), outside a hydrocarbon core of radius ~ 18 Å had to be invoked in the analysis.[18] These values are hardly reasonable considering the fact that the length of a fully extended C_{12} hydrocarbon chain equals 16.7 Å. In a later study,[19] however, these authors fitted SANS data of samples containing 0.05 M SDS or LDS in water at various concentrations of NaCl (0 ⩽ [NaCl] ⩽ 0.6 M) at 25 °C with a (two-shell) model for an ellipsoid of revolution. The data of the samples at low salt concentrations appeared to best agree with the micelles being oblate ellipsoidal whereas the data for samples at higher [NaCl], containing considerably elongated micelles, best agreed with a model for prolate aggregates. In a detailed study by Sheu and Chen[20] the growth of pure SDS and AOT micelles at 40 °C with increasing surfactant concentration was investigated using SANS. Data in the range 0.02 Å^{-1} < q < 0.25 Å^{-1} were fitted with a two-shell model for polydisperse prolate ellipsoids of revolution. In the analyses the length distribution was set equal to an exponential function with a cut-off at the lowest accessible aggregation number corresponding to a spherical micelle (the ladder model). Accordingly, the smallest micelles, for which the long axis is only slightly larger than the short axis, are approximately monodisperse which is seen from the fact that the corresponding weight-averaged and number averaged aggregation numbers as presented in ref. 20 are almost identical. In a more recent work Kumar *et al.*[21] have investigated by SANS the growth of SDS micelles in the presence of quaternary ammonium salts. The data (0.02 Å^{-1} < q < 0.18 Å^{-1}) of 0.3 M SDS solutions at 30 °C in the absence of added salt as well as at 0.1, 0.2 and 0.3 M brine were all fitted with a model for prolate ellipsoids of revolution. SDS micelles formed in 0.8 M NaCl were investigated by Almgren *et al.*[22] with static light scattering (SLS) and SANS for q values below about 0.1 Å^{-1}. We may note here that key information for the geometrical cross section structure of micelles formed by aliphatic C_{12} surfactants is contained in the range of scattering vectors 0.2–0.5 Å^{-1} [*cf.* further below].

SANS data in the range 0.025 Å^{-1} < q < 0.25 Å^{-1} from samples containing alkyldodecyltrimethylammonium bromide (C_nTAB, n = 12, 14 and 16) micelles were analysed using a (two-shell) model for prolate ellipsoids of revolution.[23] The author assumed substantial water penetration into the micelles which differed considerably between the various surfactants, *i.e.* 4.3 methylene groups mixed with water for C_{12}TAB (DTAB), 2.3 for C_{14}TAB and 2.6 for C_{16}TAB.

Recently, we have investigated micelles formed in mixtures of SDS and DTAB at 40 °C.[24,25] The best agreement with data was obtained for various models of either rigid tablet-shaped or flexible ribbon-like micelles, *i.e.* elongated bilayer fragments with a distinct thickness, width and length, respectively, and with which we could fit the data from every sample containing micelles. In the absence of added salt the micelles grow significantly both with respect to width and length as equimolar composition is approached at a fixed overall surfactant concentration. In 0.1 M NaBr the micelles were, however, seen to grow only slightly in width but very strongly with respect to the length so that long flexible ribbon-like micelles form which, in the case of SDS-rich micelles, are much too long (at least 5000 Å) for their size distribution to be determined with SANS. In both the SDS-rich and in the DTAB-rich case the micelles were seen to eventually become disk-shaped (oblate ellipsoids of revolution) below about X≡[SDS]/([SDS] + [DTAB]) = 0.05 and (above) 0.95, respectively. When our results for the geometrical dimensions of mixed SDS–DTAB micelles in 0.1 M NaBr were extrapolated to X = 0 and 1, respectively, pure SDS as well as DTAB micelles were expected to also be disk-shaped. Indeed, measurements of samples where either SDS or DTAB was the only added surfactant showed that the pure micelles at [NaBr] = 0.1 M were still shaped as disks, but with a smaller major half axis than at X = 0.05 and 0.95, respectively.[25]

The surprising discovery[24,25] that micelles formed in aqueous mixtures of SDS and DTAB are tablet-shaped have caused us to investigate more systematically the growth of pure SDS and DTAB micelles, respectively, as a function of the concentration of added salt and, in accordance, we below present the results of the corresponding SANS data analyses.

In our analyses we have considered a series of possible models for elongated aggregates: (i) Monodisperse circular cross-section with a two-step profile; (ii) polydisperse circular cross-section with a one-step profile; (iii) cylinder with swollen end caps. We also tried to fit the data of the samples containing the smallest micelles with a one-shell model for polydisperse spheres or a two-shell model for monodisperse spheres. None of these models could for physically reasonable parameters fit the data as well as a model for rods with an elliptical cross-section or a model for monodisperse oblate ellipsoids of revolution.

Materials and methods

Materials

Sodium dodecyl sulfate (SDS) (>99% purity) was obtained from Merck, dodecyltrimethylammonium bromide (DTAB) (>99%) and sodium bromide (NaBr) (>99%) from Aldrich Chemical Company and used without further purification. D_2O with 99.9 atom% D came from Aldrich Chemical Company.

Sample preparation

Stock solutions containing SDS or DTAB in pure D_2O were prepared by simply mixing either of the surfactants with D_2O to yield an overall surfactant concentration of 1.0 wt.% for SDS and the same molar concentration for DTAB (about 38 mM or 1.07 wt.%). The brine was prepared by mixing NaBr in D_2O at concentrations of 0.1, 0.2, 0.5, 0.7 and 1.0 M. Then SDS or DTAB were mixed in the various solutions of brine to yield [SDS] = 1.0 wt.% and [DTAB] = 1.07 wt.%. D_2O was chosen in order to minimise the incoherent background from hydrogen and obtain a high scattering contrast. The final samples were then obtained by means of diluting the stock solutions to 0.50 and 0.25 wt.% (or slightly above for the

DTAB solutions with identical molar concentrations) with the appropriate salt solutions. Each sample was equilibrated for at least 15 h at 40 °C before the measurements. The temperature was chosen in order to compare our results with our earlier measurements at 40 °C on mixed SDS–DTAB micelles.[25] In connection with the measurements on mixed SDS–DTAB micelles we also investigated samples of pure 5.0 wt.% SDS and DTAB, respectively, in 0.1 M NaBr as well as the diluted samples with surfactant concentrations of 2.5, 1.0 and 0.50 wt.%.

Methods

The small-angle neutron scattering (SANS) experiments were performed at the SANS instrument at the DR3 reactor at Risø National Laboratory, Denmark.[26] A range of scattering vectors $\boldsymbol{q}$ from 0.004 to 0.5 Å^{-1} was covered by four combinations of neutron wavelength (3 and 10 Å) and sample-to-detector distances (1–6 m). The different settings overlap each other in a wide regime of $\boldsymbol{q}$ values and the overlaps between different settings were optimised by three scale factors obtained by fitting to the data. The scale factors deviate somewhat from unity (less than 10%) for several reasons: (i) minor detector deadtime effects for the 1 m setting due to the high count rates; (ii) the neutron wavelength dependent correction factors we have used were measured at the D11 instrument at the Institute Laue-Langevin (ILL), Grenoble, France and cannot be expected to be absolutely correct for the instrument at Risø;[27] (iii) the data for the 6 m setting were not normalised by water at the same setting because of the very low count rate for H_2O at this sample-to-detector distance. The setting with 3 Å and 3 m sample-to-detector distance was used as the reference setting for the absolute scale which is accurate within 10%. The wavelength resolution was 18% (full width at half-maximum value).

The samples were kept in quartz cells (Hellma) with a path length of either 2, 5 or 10 mm depending on concentration. The raw spectra were corrected for background from the solvent, sample cell and other sources by conventional procedures.[27] The two-dimensional isotropic scattering spectra were azimuthally averaged, converted to an absolute scale and corrected for detector efficiency by dividing by the incoherent scattering spectra of pure water measured in a 1 mm cell.[28] The scattering intensity was furthermore normalised by dividing with the concentrations in g mL^{-1} of solute (SDS or DTAB) in the surfactant aggregates.

The average excess scattering length density per unit mass of solute $\Delta\rho_m$ was calculated using the appropriate molecular volumes and weights of the surfactant monomers ($\Delta\rho_m = -5.14 \times 10^{10}$ cm g^{-1} for SDS and $\Delta\rho_m = -6.37 \times 10^{10}$ cm g^{-1} for DTAB).[29] The molecular weight of SDS is 288.38 g mol^{-1} and of DTAB 308.35 g mol^{-1} and the molecular volumes are 410 Å^3 (SDS) and 491 Å^3 (DTAB).

Throughout the data analyses corrections were made for instrumental smearing.[26,30] For each instrumental setting the ideal model scattering curves were smeared by the appropriate resolution function when the model scattering intensity was compared with the measured one by means of least-squares methods. The parameters in the model were optimised by means of conventional least-squares analysis and the errors of the parameters were calculated by conventional methods.[31,32]

Data analyses

The excess scattering length density of an aliphatic C_{12} chain relative to a solvent consisting of D_2O is -6.8×10^{10} cm^{-2}. The difference in scattering length density between the sulfate head-group with an adjacent sodium counter-ion and D_2O is, however, much lower, *i.e.* -1.4×10^{10} cm^{-2} and for an outer shell where the head-groups are substantially mixed with solvent molecules it is much smaller. The TA^+ head-group of DTAB is largely hydrophobic and is not expected to mix with the aqueous solvent molecules. Its similarity to the hydrophobic tail of the surfactant also holds for the scattering length density which is virtually identical to that for the C_{12} chain, *i.e.* -6.8×10^{10} cm^{-2}. The bromide counter-ion has a scattering length density of -4.2×10^{10} cm^{-2} and the corresponding value for the layer outside the micelle surface, where bromide ions are substantially diluted with D_2O, is much lower. As a result, the one-shell model is a very accurate physical description of both SDS and DTAB micelles. As a matter of fact, our model fits of pure surfactant micelles presented below as well as of mixed SDS–DTAB micelles[25] and vesicles and lamellar sheets[33] using one-shell models are so good that we can not obtain any additional information using a two-shell model. In other words, we cannot distinguish between the one-shell and the two-shell models when analysing the data as the outer shell thickness in the two-shell model fit simply becomes equal to zero and the residual fit parameters identical to what is obtained with a one-shell model. Thus the data do not contain any information on the second shell and a two-shell model can only be applied if other constraints are employed on the thickness and the hydration of the head-group.[20] Similarly, since the agreement between data and model was very good it was not necessary to include any polydispersity of the cross section dimensions (thickness and width).

Hence, we can write the scattering cross section per unit mass of solute for a sample of monodisperse anisotropic particles as follows

$$\frac{d\sigma_m(\boldsymbol{q})}{d\Omega} = \Delta\rho_m^2 M\langle F^2(\boldsymbol{q})\rangle_0\left[1 + \frac{\langle F(\boldsymbol{q})\rangle_0^2}{\langle F^2(\boldsymbol{q})\rangle_0}(S(\boldsymbol{q}) - 1)\right] \quad (1)$$

where $\Delta\rho_m$ is the difference in scattering length per unit mass solute between particles and solvent and M is the molar mass of a particle. In order to account for electrostatic as well as excluded volume interactions between the comparatively small micelles we have used the decoupling approximation,[34] valid for particles with small anisotropy, together with a structure factor $S(\boldsymbol{q})$. The latter was derived by Hayter and Penfold[35] from the Ornstein–Zernike equation in the rescaled mean spherical approximation,[36] with a soft repulsive potential between two macro-ions surrounded by a diffuse double layer of counter-ions as calculated from the Poisson–Boltzmann theory.

When evaluating the geometrical shape of the smallest micelles formed in aqueous mixtures of SDS and DTAB, we obtained the best agreement between model and data using a model for a tri-axial ellipsoid with half axes a (related to the thickness) $< b$ (related to the width) $< c$ (related to the length) [*cf.* Fig. 1].[24,25] Hence, we started our analyses by fitting the data from all DTAB samples and from SDS samples with salt concentrations [NaBr] = 0.5 M and lower using this model. The orientational averaged form factor is obtained by means of integrating twice over the square of the amplitude

$$F(\boldsymbol{q}, r) = 3[\sin(\boldsymbol{q}r) - \boldsymbol{q}r\cos(\boldsymbol{q}r)]/(\boldsymbol{q}r)^3 \quad (2)$$

where

$$r(a, b, \phi, \theta) = [(a^2\sin^2\theta + b^2\cos^2\theta)\sin^2\phi + c^2\cos^2\phi]^{1/2},$$

to yield[37]

$$\langle F^2(\boldsymbol{q})\rangle_0 = \frac{2}{\pi}\int_0^{\pi/2}\int_0^{\pi/2} F^2[\boldsymbol{q}, r(a, b, c, \phi, \theta)]\sin\phi\, d\phi\, d\theta \quad (3)$$

$\langle F(\boldsymbol{q})\rangle_0$ is obtained in an analogous way by integration over the amplitudes.

When fitting the data from the samples containing SDS micelles in the absence of added salt as well as at [NaBr] = 0.1 M and DTAB micelles at [NaBr] = 0, 0.1, 0.2 and 0.5 M, we found no difference between the two larger axes, *i.e.* $b \approx c$. Hence, we refitted these data with a model for

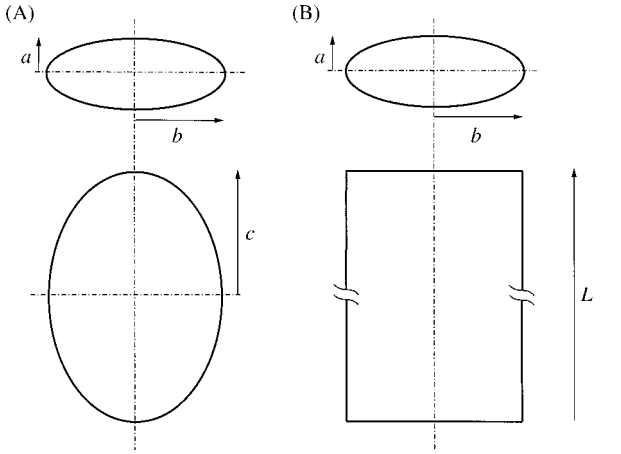

Fig. 1 Schematic representations of the model structures used for fitting the SANS data of: (A) tri-axial ellipsoids with half axes $a < b < c$. When this model was used for the smallest micelles we found that $b \approx c$ and, hence, we could fit the data with a model for oblate ellipsoids of revolution with half axes $a < b = c$. For sufficiently elongated micelles, (B) a model for polydisperse rigid rods or flexible chains of (volume-weighted) average length $\langle L \rangle$ and an elliptical cross section with half axes a and b was used.

an ellipsoid of revolution for which[38]

$$\langle F^2(\boldsymbol{q})\rangle_0 = \int_0^{\pi/2} F^2[\boldsymbol{q}, r(a, b, \phi)]\sin\,\phi\,\mathrm{d}\phi \qquad (4)$$

and $r(a, b, \phi) = [a^2 \sin^2\phi + b^2 \cos^2\phi]^{1/2}$.

As it is difficult to distinguish from our scattering data between models for oblate ellipsoids of revolution and flat cylindrical disks surrounded by a toroidal rim we have in this paper frequently used the term "disk-shape" as a common notation for both structures. The form factor of the latter structure is to our knowledge not readily available and probably difficult to calculate.

The SDS micelles formed at 0.7 M appeared to be rather elongated and polydisperse but still rigid. Hence, the corresponding data were fitted using the following scattering cross section for the rod-like structure

$$\mathrm{d}\sigma_\mathrm{m}/\mathrm{d}\Omega = \Delta\rho_\mathrm{m}^2\, P_{\mathrm{length}}(\boldsymbol{q})P_\mathrm{cs}(\boldsymbol{q})\langle M\rangle_\mathrm{w} \qquad (5)$$

where $\langle M\rangle_\mathrm{w}$ is the weight-average molar mass. In order to reduce the computation times we have written the form factor as a product of the contribution due to the length of the micelles $P_{\mathrm{length}}(\boldsymbol{q})$ and the contribution from the particle cross section $P_\mathrm{cs}(\boldsymbol{q})$. This approximation is valid since the lengths of the micelles are much larger than the cross section dimensions.[39] An elliptical cross section with half axes a and b, respectively, is described by the following expression

$$P_\mathrm{cs}(\boldsymbol{q}) = \frac{2}{\pi}\int_0^{\pi/2}\left[\frac{2B_1(\boldsymbol{q}r(a, b, \phi))}{\boldsymbol{q}r(a, b, \phi)}\right]^2 \mathrm{d}\phi \qquad (6)$$

where $r(a, b, \phi) = [a^2 \sin^2\phi + b^2 \cos^2\phi]^{1/2}$ and $B_1(x)$ is the Bessel function of first order.

The scattering function for infinitely thin polydisperse rigid rods can be written as follows

$$P_{\mathrm{length}} = \int N_\mathrm{rod}(L)L^2 S_\mathrm{rod}(\boldsymbol{q}, L, l_\mathrm{p})\mathrm{d}L \Big/ \int N_\mathrm{rod}(L)L^2\,\mathrm{d}L \qquad (7)$$

where $N_\mathrm{rod}(L)$ is the number distribution of micelles with respect to their length L and the form factor for an infinitely thin rod is given by[40]

$$S_\mathrm{rod}(\boldsymbol{q}, L) = 2\,\mathrm{Si}(\boldsymbol{q}L) - 4\sin^2(\boldsymbol{q}L/2)/(\boldsymbol{q}L)^2 \qquad (8)$$

and

$$\mathrm{Si}(x) = \int_0^x \frac{\sin t}{t}\,\mathrm{d}t \qquad (9)$$

It is difficult to take interparticle interference effects into account in the data analyses of the rather elongated SDS micelles formed at 0.7 M NaBr.[41] The repulsive double layer forces between the micelles are, however, completely negligible at such high electrolyte concentrations and the interparticle interactions are believed to be small for the comparatively dilute samples we have studied. Nevertheless the neglect of interparticle interference effects in our analyses of these aggregates may somewhat influence the quantitative outcome for the average length and length distribution of the micelles.[25]

As the SDS micelles have grown even longer at [NaBr] = 1.0 M, the corresponding scattering data could only be fitted assuming the micelles to be shaped as very long flexible ribbons. Hence, we have used the following expression for P_{length}

$$P_{\mathrm{length}} = \int N_{\substack{\mathrm{rod}\\\mathrm{worm}}}(L)L^2 S_\mathrm{KP}(\boldsymbol{q}, L, l_\mathrm{p})\mathrm{d}L \Big/ \int N_\mathrm{worm}(L)L^2\,\mathrm{d}L \qquad (10)$$

which is valid for a polydisperse collection of infinitely thin self-avoiding Kratky–Porod worm-like chains with a contour length L and persistence length l_p. The expression for the scattering function $S_\mathrm{KP}(\boldsymbol{q}, L, l_\mathrm{p})$ has been given by Pedersen and Schurtenberger.[42] In our data analysis we have assumed the number density of lengths for both rigid rods and worm-like micelles to follow a Schultz distribution

$$N_{\substack{\mathrm{rod}\\\mathrm{worm}}}(L) = \frac{L^z}{z!}\left(\frac{z+1}{\langle L\rangle_N}\right)^{(z+1)} \mathrm{e}^{-L(z+1)/\langle L\rangle_N} \qquad (11)$$

where $\langle L\rangle_N$ is the number-weighted average length of the micelles. Below we have presented our results in terms of the volume-weighted average length $\langle L\rangle = (z+2)/(z+1) \times \langle L\rangle_N$, *i.e.* the mean value as calculated from the probability distribution of finding an aggregated surfactant in a micelle of length L. The relative standard deviation, based on the volume-weighted length distribution, $\sigma_L/\langle L\rangle = (z+2)^{-1/2}$ of the polydisperse rigid SDS rods at [NaBr] = 0.7 M were found to be somewhat below unity, with large error bars, and in the corresponding model fits it was fixed to 0.95.

Results and discussion

The detailed results from our model fits are summarised in Table 1. In addition to the samples given in Table 1 we have also measured 2.5 and 5.0 wt.% SDS as well as DTAB micelles in 0.1 M NaBr (c_surf = 5.0 wt.% corresponds to about 40 times the critical micelle concentration (CMC) for SDS and to about 20 × CMC for DTAB). Small impurities of *e.g.* dodecanol in SDS would strongly influence the aggregation behaviour at surfactant concentrations close to CMC and, in particular, below CMC of the absolutely pure surfactant but this effect is expected to rapidly decrease as c_surf increases and reaches values where the amount of surfactant aggregated in micelles is significantly larger than the amount of free monomers. Moreover, we could neither for SDS nor for DTAB micelles in 0.1 M NaBr observe any significant change of the geometrical dimensions with surfactant concentration indicating that the surfactants are sufficiently pure for our purpose to determine the structure of the micelles.

In the absence of added salt as well as at low concentrations of NaBr both SDS and DTAB micelles appear to be disk-shaped. Fig. 2 shows the scattering data from a sample containing 0.50 wt.% SDS in 0.1 M NaBr together with typical examples of the best fits obtained for three different models. The corresponding fit results are given in Table 2 where we also have included the results from the best fit obtained with a model for (monodisperse) straight cylinders with hemispherical end caps[43] and monodisperse spheres. The fit of the model for spherocylinders virtually coincides with the prolate scattering curve. The model for monodisperse spheres agrees very well with data in the low $\boldsymbol{q}$ regime (as does any model for

Table 1 Results of SANS data analyses of samples where SDS and DTAB micelles form at 40 °C at various concentrations of added NaBr[a]

	[NaBr]	0.25 wt.%	0.50 wt.%	1.0 wt.%
SDS—				
	0 M	$a = 8.9$ $b = c = 19.9$ $z_{eff}/z_{id} = 0.32$ $c_{free} = 7.4$ mM $N = 42$	$a = 11.5$ $b = c = 19.8$ $z_{eff}/z_{id} = 0.28$ $c_{free} = 7.9$ mM $N = 54$	$a = 12.0$ $b = c = 20.4$ $z_{eff}/z_{id} = 0.26$ $c_{free} = 8.5$ mM $N = 60$
	0.1 M	$a = 13.4$ $b = c = 22.4$ $z_{eff}/z_{id} = 0.48$ $c_{free} = 2.3$ mM $N = 80$	$a = 13.1$ $b = c = 22.7$ $z_{eff}/z_{id} = 0.36$ $c_{free} = 3.3$ mM $N = 81$	$a = 13.1$ $b = c = 22.9$ $z_{eff}/z_{id} = 0.29$ $c_{free} = 5.4$ mM $N = 82$
	0.2 M	$a = 13.7$ $b = 23.5$ $c = 24.0$ $z_{eff}/z_{id} = 0.58$ $c_{free} = 1.9$ mM $N = 92$	$a = 13.4$ $b = 23.0$ $c = 25.0$ $z_{eff}/z_{id} = 0.42$ $c_{free} = 1.9$ mM $N = 92$	$a = 13.8$ $b = 23.0$ $c = 25.3$ $z_{eff}/z_{id} = 0.30$ $c_{free} = 4.7$ mM $N = 96$
	0.5 M	$a = 14.1$ $b = 21.5$ $c = 31.9$ $c_{free} = 1.1$ mM $N = 115$	$a = 13.9$ $b = 21.3$ $c = 33.3$ $c_{free} = 1.2$ mM $N = 118$	$a = 14.2$ $b = 21.3$ $c = 36.1$ $c_{free} = 4.0$ mM $N = 130$
	0.7 M	$a = 12.4$ $b = 19.2$ $\langle L \rangle = 250$ $\langle N \rangle = 533$	$a = 12.2$ $b = 19.6$ $\langle L \rangle = 427$ $\langle N \rangle = 914$	$a = 12.2$ $b = 20.2$ $\langle L \rangle = 537$ $\langle N \rangle = 1184$
	1.0 M	$a = 12.6$ $b = 19.4$ $l_p = 198$	$a = 12.3$ $b = 19.6$ $l_p = 219$	$a = 12.4$ $b = 19.6$ $l_p = 258$
DTAB—				
	0 M	—	$a = 8.7$ $b = c = 21.7$ $z_{eff}/z_{id} = 0.45$ $c_{free} = 14$ mM $N = 37$	$a = 12.3$ $b = c = 21.4$ $z_{eff}/z_{id} = 0.35$ $c_{free} = 17$ mM $N = 51$
	0.1 M	$a = 12.9$ $b = c = 23.2$ $z_{eff}/z_{id} = 0.24$ $c_{free} = 4.7$ mM $N = 63$	$a = 13.3$ $b = c = 23.6$ $z_{eff}/z_{id} = 0.24$ $c_{free} = 6.2$ mM $N = 67$	$a = 14.0$ $b = c = 23.7$ $z_{eff}/z_{id} = 0.22$ $c_{free} = 10$ mM $N = 72$
	0.2 M	$a = 13.6$ $b = c = 24.0$ $z_{eff}/z_{id} = 0.32$ $c_{free} = 4.1$ mM $N = 71$	$a = 13.9$ $b = c = 24.1$ $z_{eff}/z_{id} = 0.19$ $c_{free} = 5.2$ mM $N = 74$	$a = 14.0$ $b = c = 24.3$ $z_{eff}/z_{id} = 0.18$ $c_{free} = 8.9$ mM $N = 75$
	0.5 M	$a = 14.0$ $b = c = 24.7$ $c_{free} = 3.0$ mM $N = 78$	$a = 14.3$ $b = c = 24.8$ $c_{free} = 3.9$ mM $N = 81$	$a = 14.5$ $b = c = 25.0$ $c_{free} = 7.9$ mM $N = 83$
	0.7 M	$a = 14.5$ $b = 23.0$ $c = 27.2$ $c_{free} = 2.4$ mM $N = 83$	$a = 14.6$ $b = 23.0$ $c = 27.2$ $c_{free} = 3.7$ mM $N = 83$	$a = 14.7$ $b = 23.0$ $c = 27.7$ $c_{free} = 9.7$ mM $N = 85$
	1.0 M	$a = 14.7$ $b = 21.8$ $c = 29.5$ $c_{free} = 1.7$ mM $N = 86$	$a = 14.9$ $b = 22.3$ $c = 29.8$ $c_{free} = 3.0$ mM $N = 90$	$a = 14.9$ $b = 22.4$ $c = 30.2$ $c_{free} = 7.0$ mM $N = 92$

[a] The data of samples containing SDS micelles at [NaBr] $\leqslant 0.5$ M and DTAB micelles were fitted with a model for monodisperse tri-axial ellipsoids with half axes a (related to the thickness) $< b$ (related to the width) $< c$ (related to the length). The data of the samples for which $b \approx c$ were refitted with a model for oblate ellipsoids of revolution with half axes a and $b = c$. SDS micelles at [NaBr] = 0.7 M were fitted with a model for polydisperse rigid rods with a volume-weighted average length $\langle L \rangle$ and an elliptical cross section with half axes a and b, and SDS micelles at [NaBr] = 1.0 M with a model for polydisperse self-avoiding worm-like chains with a persistence length l_p and cross section half axes a and b. The relative standard deviation, based on the volume-weighted size distribution, $\sigma_L/\langle L \rangle$ appeared to be somewhat below unity for the rigid rods formed in 0.7 M NaBr and in the corresponding model fits $\sigma_L/\langle L \rangle$ was fixed to 0.95. The ribbon-like micelles were too large for their size distribution to be determined from our SANS data. All spatial dimensions are given in angstroms (Å). The structure factor necessary for fitting the data at lower salt concentrations accounts for the comparatively large double layer interactions between macro-ions with an effective charge z_{eff}. The ideal charge z_{id} is the charge of a micelle for which the counter-ions are fully dissociated. The aggregation number N was calculated for SDS micelles assuming only the hydrocarbon chain of each surfactant (molecular volume equalling 351 Å^3) to contribute to the scattering intensity and for DTAB micelles assuming the whole ionic species DTA^+ (molecular volume equalling 460 Å^3) to contribute to the scattering intensity. The absolute intensities are only accurate within 10% which means an error of the calculated values of c_{free} of 1 mM for the samples at 0.25 wt.%, 2 mM at 0.50 wt.% and 4 mM at 1.0 wt.%. c_{free} for the SDS samples at [NaBr] = 0.7 M and 1.0 M could not be calculated accurately as particle interference effects were omitted in the analyses. The statistics of the data for the comparatively diluted samples of small particles at [SDS] = 0.25 and 0.50 wt.% and [DTAB] = 0.50 wt.% in the absence of added salt were not as good and, hence, the results of these fits were not as reliable as for the other samples.

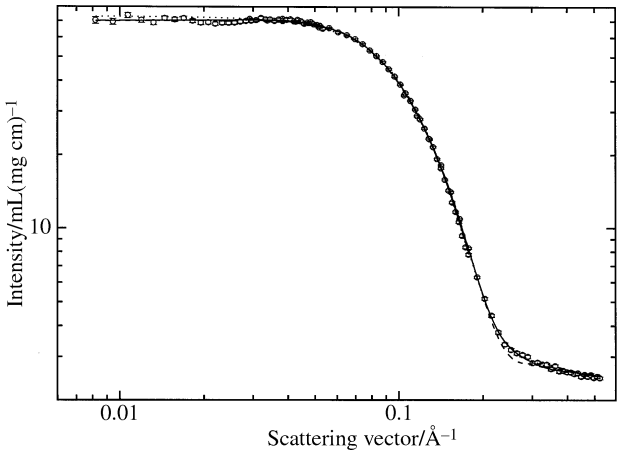

Fig. 2 Normalised scattering intensity as a function of the scattering vector $\boldsymbol{q}$ for a sample where [SDS] = 0.50 wt.% and [NaBr] = 0.1 M. Individual symbols represent data obtained with different combinations of neutron wavelength and sample–detector distance. The solid lines represent the best available fit with a model for monodisperse oblate ellipsoids of revolution, the dashed lines the best available fit with a model for monodisperse prolate ellipsoids of revolution and the dotted lines the best available fit with a model for polydisperse spheres. The results of the model fits are given in Table 2. The agreements of the fits as measured by[31] χ^2 are 2.3, 3.9 and 3.8, respectively. When the data are fitted with two-shell models for monodisperse particles the outer thickness becomes equal to zero and the same fit results are obtained as with the corresponding one-shell models.

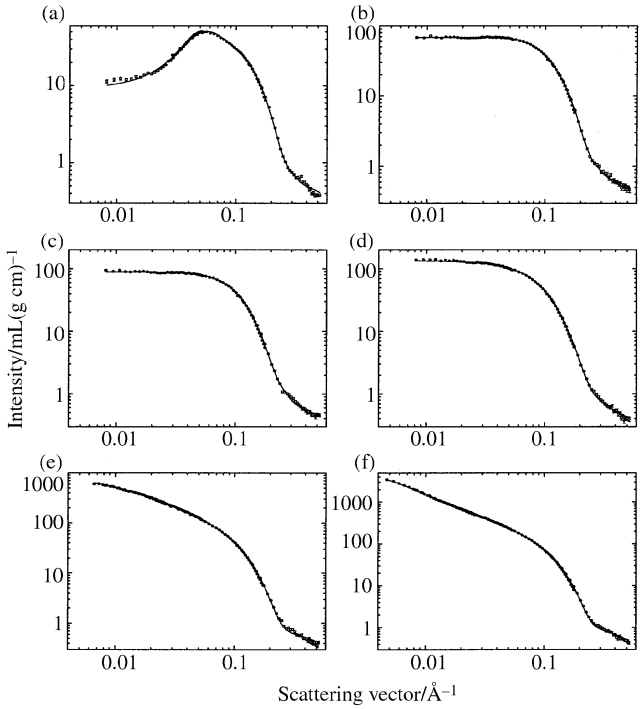

Fig. 3 Normalised scattering intensity as a function of the scattering vector $\boldsymbol{q}$ for samples with a concentration of added salt (*a*) [NaBr] = 0, (*b*) [NaBr] = 0.1 M, (*c*) 0.2 M, (*d*) 0.5 M, (*e*) 0.7 M and (*f*) 1.0 M at an overall surfactant concentration of [SDS] = 0.50 wt.% except for (*a*) where [SDS] = 1.0 wt.%. Individual symbols represent data obtained with different combinations of neutron wavelength and sample detector distance. The lines represent the results from fits with models for monodisperse oblate ellipsoids of revolution (*a* and *b*), monodisperse tri-axial ellipsoids (*c* and *d*), polydisperse rigid rods with elliptical cross section (*e*) and self-avoiding worm-like ribbons with elliptical cross section (*f*). The results of the model fits are given in Table 1. The agreement of the fits as measured by χ^2 is 7.1 ([NaBr] = 0), 2.3 ([NaBr] = 0.1 M), 4.1 ([NaBr] = 0.2 M), 2.5 ([NaBr] = 0.5 M), 5.0 ([NaBr] = 0.7 M) and 3.7 ([NaBr] = 1.0 M).

monodisperse aggregates) but deviates considerably from the scattering data at high $\boldsymbol{q}$ values. Good agreement between a model for *polydisperse* spheres and data in the high $\boldsymbol{q}$ regime can be obtained assuming the relative standard deviation with respect to the micelle radius R_s to be as large as $\sigma_{Rs}/\langle R_s\rangle = 0.25$. There is, however, a coupled dependence between the cross section structure and the overall size for spherical aggregates and, as a consequence, the large polydispersity of the micelles influence the scattering behaviour at low $\boldsymbol{q}$ values resulting in a rather poor agreement between data and model in the regime below about $\boldsymbol{q} = 0.08$ Å^{-1} where the scattering behaviour is typical of that for *monodisperse* particles. For a sample containing SDS or DTAB in the absence of added salt the agreement between the polydisperse sphere model and data is even worse since the pronounced peak in the scattering data in Fig. 3a becomes completely blurred for large variances with respect to R_s. We may also note that the largest radius of the polydisperse spheres given in Table 2, $\langle R_s\rangle + 2\sigma_{Rs} \approx 24$ Å, is much larger than a fully extended C_{12} chain (=16.7 Å) which means that there must be a hole at the centre of the micelles. A similar scattering curve to that for polydisperse spheres can be obtained with a two-shell model for monodisperse spheres assuming unphysical values of the relative scattering length density between inner and outer shell and the outer shell thickness, respectively.

Table 2 Results of SANS data analyses of a sample containing 0.5 wt.% SDS in 0.1 M NaBr using models for monodisperse oblate ellipsoids of revolution with half axes *a* and *b*, prolate ellipsoids of revolution with half axes *a* and *b*, cylinders of length *L* and radius R_c with hemi-spherical end caps of radius R_c [*cf.* ref. 43], monodisperse spheres with radius R_s and polydisperse spheres with (number-weighted) average radius $\langle R_s\rangle$[a]

Monodisperse oblate ellipsoids of revolution	Monodisperse prolate ellipsoids of revolution	Mondisperse spherocylinders	Monodisperse spheres	Polydisperse spheres
$a = 13.1$	$a = 26.9$	$R_c = 15.4$	$R_s = 19.1$	$\langle R_s\rangle = 16.0$
$b = 22.7$	$b = 16.1$	$L = 18.3$	$z_{eff}/z_{id} = 0.28$	$\sigma_{Rs}/\langle R_s\rangle = 0.25$
$z_{eff}/z_{id} = 0.36$	$z_{eff}/z_{id} = 0.39$	$z_{eff}/z_{id} = 0.39$	$N = 83$	$z_{eff}/z_{id} = 0.22$
$N = 81$	$N = 83$	$N = 82$	$\chi^2 = 18$	$\langle N\rangle = 48$
$\chi^2 = 2.3$	$\chi^2 = 3.9$	$\chi^2 = 3.6$		$\chi^2 = 3.8$

[a] All spatial dimensions are given in angstroms (Å). The structure factor used accounts for the double layer interactions between macro-ions with an effective charge z_{eff}. The ideal charge z_{id} is the charge of a micelle for which the counter-ions are fully dissociated. For the polydisperse spheres the structure factor was incorporated using the decoupling approximation. The aggregation number *N* was calculated assuming only the hydrocarbon chain of each surfactant (molecular volume equalling 351 Å^3) to contribute to the scattering intensity. The agreements between data and model fits are measured by χ^2.[31] When fitting the data with two-shell models for an ellipsoid of revolution or a spherocylinder the outer thickness becomes equal to zero and the same fit results are obtained as with the corresponding one-shell models. The agreement between a model for monodisperse spheres can be substantially improved, in a similar way as when polydispersity is allowed for, by invoking an outer concentric shell to the sphere (two-shell model) and assuming unphysical values of the relative scattering length density between inner and outer shell and the outer shell thickness.

The scattering behaviours for an oblate and a prolate ellipsoid of revolution (or a spherocylinder) are similar at low q values which contain information about overall size, polydispersity and intermicellar interactions (surface charge) [*cf.* Fig. 2 and Table 2]. As a result, the corresponding parameters are approximately independent of the geometry of the micelles assumed in the model fit [*cf.* Table 2]. In accordance, our obtained values for the aggregation numbers of SDS micelles in the absence of added salt at 0.5 and 1.0 wt.% [*cf.* Table 1] agrees very well with what was obtained by Sheu *et al.*[20] at the same temperature (40 °C) with a model for prolate ellipsoids of revolution. However, the scattering behaviour between the two models differs significantly in the regime 0.2 $Å^{-1} < q < 0.3$ $Å^{-1}$, where good agreement with data could only be obtained assuming the micelles to be shaped as oblate disks. SANS data of samples containing SDS in the absence of added salt have previously been analysed using a model for prolate ellipsoids of revolution.[20,21] However, model fits assuming the aggregates to be shaped as disks or oblate ellipsoids of revolution were not attempted in either of these works and, moreover, large parts of the q-regime where the models for oblate and prolate ellipsoids of revolution are different were not measured.

The prolate model cannot be improved by using a two-shell model even with unphysical values of the relative scattering length density between inner and outer shell and thickness of the outer shell. This is so because any improvement in the high q-range deteriorates the agreement between model and data in the low q-range in a similar way as with the polydisperse sphere model. As a result, the thickness of the outer layer becomes equal to zero when the data are fitted with a two-shell model. This means that it is not possible to experimentally determine the hydration number of the aggregated head-groups from the scattering data. Accordingly, when a two-shell model is used to fit the data (as was done in ref. 20) where the thickness of the outer shell is set to some reasonable value and the corresponding scattering length density to its appropriate value, the contribution to the scattering from the outer shell would be negligible and the fit results identical to that obtained from the corresponding one-shell model as presented in Table 2.

Reasonable fits could be obtained for the smallest micelles with a model for cylinders with swollen end-caps but this model could not at all fit the data of the comparatively large SDS micelles found at [NaBr] = 0.7 and 1.0 M. Regarding spherical or cylindrical micelles with protruding monomers at the aggregate surface, which can be considered as the result of the exchange of monomers between the micelles and the surrounding solution, we have performed model calculations on a modified version of the model by Pedersen and Gerstenberg[44] for particles with radial hairs. In accordance, about half of the aggregated monomers have to experience protrusions with an average magnitude of about 8 Å to yield a scattering curve resembling the ones we have observed. Considering the very large free energies connected with exposing the hydrocarbon chains to the water (about 15–20 kT which can be estimated from the surface interfacial tension the macroscopic value of which is 50 mJ m^{-2}) this possibility can be ruled out. Hence, models for rigid oblates or tablets or flexible ribbon-like micelles are the only ones that, with physically reasonable values of the fit parameters, are able to fit the data from all pure SDS and DTAB solutions as well as all mixed SDS–DTAB solutions[24,25] containing micelles.

Our result for the shape of the smallest micelles agrees very well with the conclusion arrived at by Corti and Degiorgio[45] that the diffusion behaviour of SDS micelles in 0.1 M NaCl at 25 °C is consistent with that for oblate ellipsoidal particles ($b/a = 1.8$) rather than prolates. However, since it is well-known that SDS micelles become considerably elongated at higher electrolyte concentrations it has generally just been assumed that the micelles are shaped as prolates or elongated cylinders with a circular cross section.

Examples of SANS data together with model fits of samples containing SDS micelles formed at various concentrations of added NaBr are given in Fig. 3. The SDS micelles become tablet-shaped at about [NaBr] = 0.2 M where the micelles start to grow strongly in length, whereas the width slightly decreases, as the concentration of added salt is further increased [*cf.* Fig. 4]. Nevertheless, all elongated micelles have an elliptical rather than a circular cross section. The lengths of the rigid SDS micelles found at [NaBr] = 0.7 M are large and the aggregates appear to be rather polydisperse in the length direction and at [NaBr] = 1.0 M flexible ribbons form that are too long for their size to be determined by our SANS equipment [*cf.* Table 1]. The SDS samples at [NaBr] = 1.0 M were seen to be rather viscous as compared with the other samples.

A typical example of the large difference in scattering behaviour at high q values between a model for elongated micelles with a circular and non-circular cross section, respectively, is demonstrated in Fig. 5. As the form factor of the elongated SDS micelles at [NaBr] = 0.7 and 1.0 M is separated into a length part and a cross section part [*cf.* eqn. (5)], the

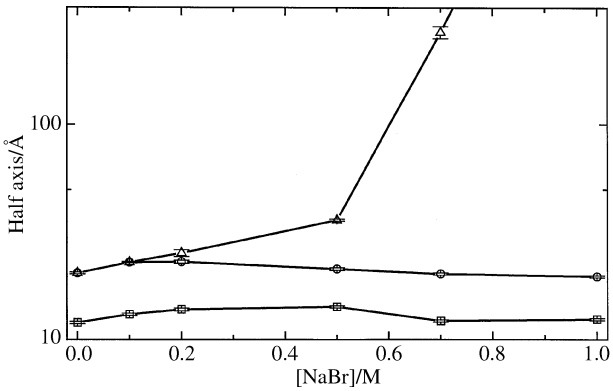

Fig. 4 Half axes related to the thickness a (squares), width b (circles) and length c (triangles), with error bars, of SDS micelles formed in 1.0 wt.% surfactant solutions plotted against the concentration of NaBr. For the polydisperse micelles formed at 0.7 M the (triangular) symbol represents half the volume weighted average length $\langle L \rangle/2$. Note the logarithmic scale of the vertical axis.

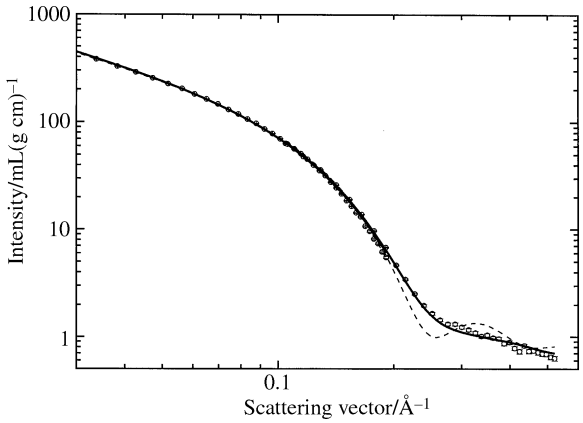

Fig. 5 Normalised scattering intensity as a function of the scattering vector q in the high q range for [SDS] = 0.50 wt.% and [NaBr] = 1.0 M. Individual symbols represent data obtained with different combinations of neutron wavelength and sample detector distance. The solid lines represent the best available fit assuming an elliptical cross section resulting in half-axes $a = 12.3$ Å and $b = 19.6$ Å. The dashed lines represent the best available fit assuming a circular cross section giving a cylinder radius of 15.5 Å. The agreement of the former fit in the interval $0.1 < q/Å^{-1} < 0.6$ as measured by χ^2 equals 10.0 and of the latter $\chi^2 = 53.3$.

obtained values of the micelle size and polydispersity, included in P_{length}, are determined by the scattering behaviour in the low q-regime and are independent on the structure of the cross section as included in P_{cs}. The deviation between data and models for prolate ellipsoids of revolution or cylinders at high q-values increases systematically with the size of the micelles (*cf.* Figs. 2 and 5) whereas the cylinder radius as obtained in the corresponding model fits is rather constant ($a \approx 16$ Å for SDS and $a \approx 18$ Å for DTAB) with respect to [NaBr].

We could, however, obtain an agreement with data as good as with a model for a micelle with an elliptical cross section by assuming a standard deviation of the cylinder radius as large as $\sigma_{R_c}/\langle R_c \rangle = 0.20$. This corresponds to a maximum cylinder radius of about 20 Å (that is equal to the half axis b related to the width of the micelles as obtained from our model fits assuming an elliptical cross section). This value is much larger than expected as a fully extended C_{12} hydrocarbon chain equals 16.7 Å and one would expect neither a hole in the centre of the micelles nor the hydrocarbon chains to be fully stretched because of the large difference in chain conformation entropy between stretched and non-stretched chains.[2,3]

According to previous model calculations[6] the variance in cylinder radius is believed to be rather small, *i.e.* $\sigma_{R_c}/\langle R_c \rangle = 0.01$, mainly due to the free energy contribution accounting for the conformational entropy of the hydrocarbon chains. Moreover, when investigating the various bilayer structures formed from mixtures of SDS and DTAB we did not observe any large deviations from the models at high q assuming a non-varying (one-shell) bilayer thickness.[33] The same free energy contributions determine the equilibrium radial distance of the cross section for spherical, cylindrical and planar geometries, respectively, and, hence, its polydispersity is expected to vary only slightly with geometry.[5–7]

Agreement between data and a two-shell model for a circular cross-section could only be obtained assuming unphysical values of the fit parameters. Typical (and unreasonable) values for the relative scattering length density between inner and outer shell and the outer shell thickness of SDS micelles at [NaBr] = 0.7 and 1.0 M are $\rho_i/\rho_o \approx 0.25$ and 12 Å, respectively, for the best fit with a two-shell cylinder model.

Some of the samples containing mixed SDS–DTAB tablet-shaped micelles were also measured at the D22 SANS instrument (10% wavelength resolution) at the ILL, Grenoble, France and we obtained the same results as we did at Risø.[25] Moreover, inverted worm-like micelles for which the cross-section was found to be circular have previously been measured at Risø as well as at the ILL.[41,46] Hence, we can safely exclude the possibility that the determined oblate shape of small micelles and elliptical cross section of elongated micelles is a result of instrumental effects or of the poorer wavelength resolution of the SANS instrument at Risø as compared with the instrument at the ILL. The wavelength resolution should in any case not be expected to influence the results as we include full instrumental correction in our data analysis.

Interparticle interference effects were not included in the models for the polydisperse rigid or flexible elongated SDS micelles at [NaBr] = 0.7 M and 1.0 M, respectively (*cf.* above). As a result, the rate with which the micelle size increases with surfactant concentration appears to be less in our results than what had been obtained if interparticle interference effects were taken into account in our analyses.[41] Likewise, the appeared increase of the persistence length of the ribbon-like micelles with surfactant concentration [*cf.* Table 1] is most likely mainly due to the neglect of interparticle interference effects in the corresponding model fits. When the persistence length is plotted against the surfactant concentration and extrapolated to zero we find that l_p ([SDS] = 0) = 178 Å. This value is in very good agreement with the results obtained by Jerke *et al.* for inverse lecithin worm-like micelles[41] and for (uncharged) pure $C_{16}E_6$ micelles[47] but somewhat lower than the value 280 Å found for mixed $C_{16}E_6$–$C_{16}SO_3Na$ micelles in 10 mM NaCl.[47] The persistence length is expected to increase with the cross section dimension, *i.e.* hydrocarbon chain length, and surface charge density of the micelles and decrease for charged micelles with increasing concentration of added salt. This is in agreement with experimental observations.

Examples of scattering data together with model fits for DTAB micelles in different concentrations of NaBr are given in Fig. 6. In contrast to the SDS micelles, DTAB micelles grow only slightly as NaBr is added to the solutions [*cf.* Fig. 7]. At 0.5 M NaBr the micelles are still oblate ellipsoids of revolution whereas they have become slightly elongated at 0.7 M. Evidently, the different behaviour between the growths of SDS and DTAB micelles upon addition of salt cannot be explained only by arguments using an electrostatic mean-field theory such as the Poisson–Boltzmann theory. Hence, specific contributions due to the difference in head-groups and counter-ions between SDS and DTAB must be significant for the rate with which the micelles grow as a function of electrolyte concentration.

There is a slight increase of the size of the comparatively small disk-shaped micelles with surfactant concentration which become more significant above 0.5 M NaBr where the micelles begin to grow in length. The growth of the micelles is a result of the decreasing entropy of mixing aggregates and solvent, the contribution of which favours small aggregates, with increasing surfactant concentration. As the work of bringing *an extra surfactant monomer* into a micelle as com-

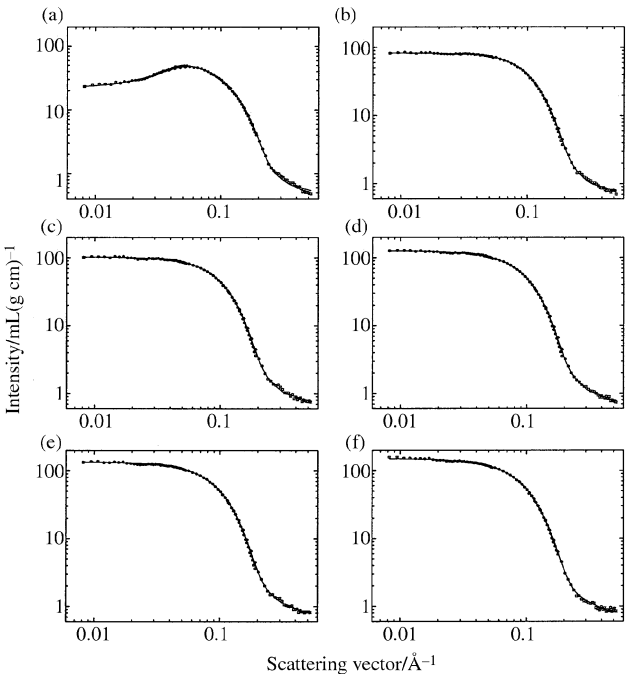

Fig. 6 Normalised scattering intensity as a function of the scattering vector q for samples with a concentration of added salt (*a*) [NaBr] = 0, (*b*) [NaBr] = 0.1 M, (*c*) [NaBr] = 0.2 M, (*d*) [NaBr] = 0.5 M, (*e*) [NaBr] = 0.7 M and (*f*) and [NaBr] = 1.0 M at an overall surfactant concentration of [DTAB] = 0.50 wt.% except for (*a*) where [DTAB] = 1.0 wt.%. Individual symbols represent data obtained with different combinations of neutron wavelength and sample detector distance. The lines represent the results from fits with models for monodisperse oblate ellipsoids of revolution (*a*, *b*, *c* and *d*) and monodisperse tri-axial ellipsoids (*e* and *f*). The results of the model fits are given in Table 1. The agreement of the fits as measured by χ^2 is 5.3 (NaBr] = 0), 3.6 (NaBr] = 0.1 M), 4.4 ([NaBr] = 0.2 M), 5.5 ([NaBr] = 0.5 M), 5.6 ([NaBr] = 0.7 M) and 3.7 ([NaBr] = 1.0 M). Note the smaller influence of the structure factor, which brings down the intensity at low q values, for DTAB micelles in the absence of added salt compared with the corresponding case for SDS [*cf.* Fig. 3a] due to the larger free monomer concentration in the former case.

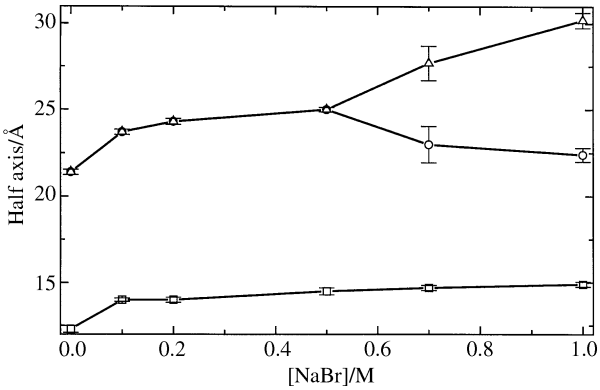

Fig. 7 Half axes related to the thickness *a* (squares), width *b* (circles) and length *c* (triangles), with error bars, of DTAB micelles formed in 1.0 wt.% surfactant solutions plotted against the concentration of NaBr. The error bars become increasingly larger as the difference between length and width decreases and the two parameters become more correlated to each other.

pared to the work per monomer of forming *an extra micelle* is more favourable for a linear[6] than for a non-linear[5,7] micelle, the rate of growth becomes larger for the former type of aggregate. As a consequence, a rapid growth with surfactant concentration is always associated with a high polydispersity of the micelles.[48]

The thicknesses of the micelles are of the same magnitude as obtained for micelles[25] and various bilayer structures[33] formed from mixtures of SDS and DTAB, *i.e.* substantially less than a fully extended hydrocarbon C_{12} chain. This is consistent with a comparatively high conformational entropy for non-stretched hydrocarbon chains packed in a liquid-like layer.[2,3] There is a tendency that the micelles become thicker with increasing [NaBr] at low salt concentrations indicating that the electrostatic free energy contribution is important in this regime. However, the thickness of the very long SDS micelles at higher electrolyte concentrations tends to decrease with [NaBr]. This can be explained as a result of a change in chain conformational entropy with decreasing curvature of the micelles since, in accordance with this free energy contribution, the optimal layer thickness decreases with geometry in the following order: sphere > cylinder > plane.[3]

In addition to the parameters given in Table 1 we also optimised an (apparent) average molar mass of the aggregates and a residual background when fitting the data. Typical values of the latter, which are common for all four neutron wavelength/sample-to-detector settings, are 0.1–0.7 mL g^{-1} cm^{-1}. The aggregation numbers N included in Table 1 were calculated from the micelle volumes assuming that only the hydrocarbon C_{12} tail ($v = 351$ Å^3) of SDS contributes to the scattering intensity of SDS micelles whereas also the TA^+ head-group ($v = 109$ Å^3) of DTAB contributes to the scattering intensity of DTAB micelles in accordance with arguments given above.

An apparent aggregation number N_{app} can be calculated from the molar weights of the micelles, obtained from the absolute intensities, and the molecular weights. When N and N_{app} are compared for samples with low concentrations of added salt, it is evident that the amount of surfactant aggregated in the micelles contributing to the scattering intensity is substantially less than the amount of added surfactant. The reason for this is that a certain amount of surfactant coexists with the micelles as free monomers, the chemical potential of which $\mu_{free} \propto \log c_{free}$ (approximately) equals the chemical potential of the aggregated surfactant μ_{mic}. We have calculated N_{app} by roughly using the value for the molecular weight of the entire surfactant molecule (without including any D_2O molecules). However, it appears that the resulting values of N_{app} are rather independent of the chosen molecular structure as the molecular weight of the entire micelle, determined by the excess scattering length density of the surfactant, varies in a similar way as the surfactant molecular weight when counter-ion and solvent molecules are added to the surfactant. The free monomer concentrations c_{free} as calculated from the difference between N_{app} and N are given in Table 1. The values we have obtained are reasonable considering the fact that the critical micelle concentration of SDS is about 8 mM at 25 °C in the absence of added salt and the corresponding value for DTAB is about 16 mM. The expected 10% error on the absolute intensity leads, however, to a relatively large error on c_{free}. c_{free} is seen to decrease with increasing concentration of added salt as μ_{mic} is reduced as a result of a decreasing electrostatic free energy contribution. A certain increase of the free monomer concentration as the entropy of mixing micelles and solvent decreases with increasing overall surfactant concentration is expected for a collection of non-interacting surfactant micelles,[5,49] a trend that is expected to become even more evident as repulsive intermicellar interactions are taken into account.

We may note that our procedure to determine N and c_{free} is slightly different from the one usually used. The usual procedure is to fit the aggregation number and some parameters describing the shape of the micelle. The aggregation number is used for calculating the volume of the micelle (or of the two components, core and shell, for a two-shell model). An overall scale is used for getting the data to fit on an absolute scale; a value close to unity is taken as evidence that the model fits the data on an absolute scale. Although the two approaches deviate somewhat in the procedures, they are for all practical purposes equivalent.

A better agreement between model and data was obtained as the amount of free monomers was subtracted from the overall surfactant concentration when the particle volume fraction used in the calculations of the structure factor was evaluated. The hard sphere radius was set equal to the radius of a sphere with the same volume as the anisotropic micelle. The electrolyte concentrations in the samples in the absence of added NaBr were found to be about 9 mM for SDS and 18 mM for DTAB corresponding to Debye lengths of about 40 and 30 Å, respectively. At higher concentrations of added salt the electrolyte concentration was set equal to [NaBr]. The Debye length at 0.1 M NaBr is about 12 Å and decreases to about 4 Å upon further increasing the salt concentration to 1.0 M. The effective charge z_{eff} as obtained from our analyses divided by the charge of a fully dissociated macro-ionic micelle z_{id} is also given in Table 1. The ratio z_{eff}/z_{id} is found to be in-between 0.18 and 0.58. We may stress here that z_{eff} is an effective charge as the structure factor is calculated from the PB approximation assuming, among other things, a smeared out surface charge of the micelles and infinitely small counterions (point charges). Only hard-sphere interactions between SDS (neglected at [NaBr] = 0.7 and 1.0 M) and DTAB micelles were seen to contribute to $S(q)$ for concentrations of added salt [NaBr] equal and larger than 0.5 M and, hence, z_{eff} could not be determined for these samples.

Conclusion

In the present paper on pure SDS and DTAB micelles as well as in a recent study of mixed SDS–DTAB surfactant micelles (refs. 24 and 25) we have been able to fit the SANS data for a large number of samples containing micelles in the entire relevant regime of scattering vectors using models for oblate or tablet-shaped micelles. A series of other possible models were tried for the elongated micelles: (1) monodisperse cross section with a two-step profile; (2) polydisperse circular cross section with a one step profile; (3) cylinder with swollen end caps. Models for monodisperse or polydisperse spheres were also tried for the smallest micelles. However, none of these models could for physically reasonable parameters fit the data as well

as models for tri-axial ellipsoids rods with an elliptical cross section or monodisperse oblate ellipsoids of revolution. To obtain good agreements with the scattering data of samples containing considerably elongated micelles polydispersity in the length direction and, for the longest micelles, flexibility must be included in the models. We neither need to, *ad hoc*, invoke a large variance of the cross section radius nor substantial water penetration into the aggregates nor a hole in the centre of the micelles as has frequently been done when common geometrical structures were used for analysing small-angle scattering data of samples containing micelles.

When evaluating the structure of SDS and DTAB micelles as a function of the concentration of added NaBr we did not observe the frequently referred sphere-to-cylinder transition. In contrast, both SDS and DTAB micelles formed in 0.25–1.0 wt.% surfactant solutions are found to be disk-shaped in the absence of added salt at 40 °C. At low concentrations of added salt the disk radius increases with [NaBr] and, at a given concentration, tablet-shaped micelles emerge as the micelles start to grow significantly with respect to the length at almost constant width and thickness. The growth of the micelles is more pronounced for the SDS case, in which the micelles at [NaBr] = 1.0 M are found to be flexible rather than rigid and with a size too large to be determined with our SANS equipment. DTAB micelles formed at the same electrolyte concentration are only about $2c = 60$ Å long. The results presented in earlier SANS studies of SDS micelles are contradictory.[17,19,20] Scattering vectors in the regime $q > 0.25$ Å^{-1}, which contains important information about the structure of surfactant micelles, were not measured in refs. 19 and 20 and the scattering behaviour for polydisperse aggregates in the regime of low q-values was not investigated in ref. 17. As we in our analyses have compared the agreement for several conceivable models with scattering data in the entire relevant q-regime we believe the problem of the structure of SDS micelles to be finally settled with this work.

Acknowledgements

M.B. was supported by a Marie Curie Fellowship from the Training and Mobility of the Researches (TMR) Programme of the European Union.

References

1 C. Tanford, *The hydrophobic effect*, Wiley, New York, 1980.
2 D. W. R. Gruen and E. H. B. Lacey, in *Surfactants in solution*, ed. K. Mittal and B. Lindman, Plenum, New York, 1984, vol. 1, p. 279.
3 D. W. R. Gruen, *J. Phys. Chem.*, 1985, **89**, 153.
4 I. Szleifer, D. Kramer and A. Ben-Shaul, *J. Chem. Phys.*, 1990, **92**, 6800.
5 J. C. Eriksson, S. Ljunggren and U. Henriksson, *J. Chem. Soc., Faraday Trans. 2*, 1985, **81**, 833.
6 J. C. Eriksson and S. Ljunggren, *J. Chem. Soc., Faraday Trans. 2*, 1985, **81**, 1209.
7 S. Ljunggren and J. C. Eriksson, *J. Chem. Soc., Faraday Trans. 2*, 1986, **82**, 913.
8 N. A. Mazer, G. B. Benedek and M. C. Carey, *J. Phys. Chem.*, 1976, **80**, 1075.
9 O. Söderman, M. Jonströmer and J. van Stam, *J. Chem. Soc. Faraday Trans.*, 1993, **89**, 1759.
10 M. Törnblom, U. Henriksson and M. Ginley, *J. Phys. Chem.*, 1994, **98**, 7041.
11 J. B. Hayter and J. Penfold, *J. Chem. Soc, Faraday Trans. 1*, 1981, **77**, 1851.
12 J. B. Hayter and J. Penfold, *Colloid Polym. Sci.*, 1983, **261**, 1022.
13 D. Bendedouch and S. H. Chen, *J. Phys. Chem.*, 1983, **87**, 1653.
14 D. Bendedouch and S. H. Chen, *J. Phys. Chem.*, 1984, **88**, 648.
15 E. Y. Sheu, C. F. Wu and S. H. Chen, *J. Phys. Chem.*, 1986, **90**, 4179.
16 D. Bendedouch and S. H. Chen, *J. Phys. Chem.*, 1983, **87**, 153.
17 B. Cabane, R. Duplessix and T. Zemb, *J. Phys.*, 1985, **46**, 2161.
18 S. S. Berr, M. J. Coleman, R. R. M. Jones and J. S. Johnson, Jr., *J. Phys. Chem.*, 1986, **90**, 6492.
19 S. S. Berr and R. R. M. Jones, *Langmuir*, 1988, **4**, 1247.
20 E. Y. Sheu and S. H. Chen, *J. Phys. Chem.*, 1988, **92**, 4466.
21 S. Kumar, S. L. David, W. K. Aswal, P. S. Goyal and Kabir-ud-Din, *Langmuir*, 1997, **13**, 6461.
22 M. Almgren, J. C. Gimel, K. Wang, G. Karlsson, K. Edwards, W. Brown and K. Mortensen, *J. Colloid Interface Sci.*, 1998, **202**, 222.
23 S. S. Berr, *J. Phys. Chem.*, 1987, **91**, 4760.
24 M. Bergström and J. S. Pedersen, *Langmuir*, 1999, **15**, 2250.
25 M. Bergström and J. S. Pedersen, *J. Phys. Chem. B*, in press.
26 J. S. Pedersen, *J. Phys. IV*, *Coll. C8*, 1993, **3**, 491.
27 J. P. Cotton, in *Neutron, X-Ray and Light Scattering: Introduction to an Investigative Tool For Colloidal and Polymeric Systems*, ed. P. Lindner and T. Zemb, North-Holland, Amsterdam, 1991.
28 G. D. Wignall and F. S. Bates, *J. Appl. Crystallogr.*, 1986, **20**, 28.
29 Y. Chevalier and T. Zemb, *Rep. Prog. Phys.*, 1990, **53**, 279.
30 J. S. Pedersen, D. Posselt and K. Mortensen, *J. Appl. Crystallogr.*, 1990, **23**, 321.
31 B. R. Bevington, in *Data Reduction and Error Analysis for Physical Sciences*, McGraw-Hill, New York, 1969.
32 J. S. Pedersen, *Adv. Colloid Interface Sci.*, 1997, **70**, 171.
33 M. Bergström, J. S. Pedersen, P. Schurtenberger and S. U. Egelhaaf, *J. Phys. Chem. B*, in press.
34 M. Kotlarchyk and S. H. Chen, *J. Chem. Phys.*, 1983, **79**, 2461.
35 J. B. Hayter and J. Penfold, *Mol. Phys.*, 1981, **42**, 409.
36 J. P. Hansen and J. B. Hayter, *Mol. Phys.*, 1982, **46**, 651.
37 P. Mittelbach and G. Porod, *Acta Phys. Austriaca*, 1962, **15**, 122.
38 A. Guinier, *Ann. Phys.*, 1939, **12**, 161.
39 J. S. Pedersen and P. Schurtenberger, *J. Appl. Crystallogr.*, 1996, **29**, 646.
40 T. Neugebauer, *Ann. Phys.* (*Leipzig*), 1943, **42**, 509.
41 G. Jerke, J. S. Pedersen, S. U. Egelhaaf and P. Schurtenberger, *Phys. Rev. E*, 1997, **56**, 5772.
42 J. S. Pedersen and P. Schurtenberger, *Macromolecules*, 1996, **29**, 7602.
43 S. Cusack and A. Miller, *J. Mol. Biol.*, 1981, **145**, 525.
44 J. S. Pedersen and M. C. Gerstenberg, *Macromolecules*, 1996, **29**, 1363.
45 M. Corti and V. Degiorgio, *Chem. Phys. Lett.*, 1978, **53**, 237.
46 P. Schurtenberger, G. Jerke, C. Cavaco and J. S. Pedersen, *Langmuir*, 1996, **12**, 2433.
47 G. Jerke, J. S. Pedersen, S. U. Egelhaaf and P. Schurtenberger, *Langmuir*, 1998, **14**, 6013.
48 J. N. Israelachvili, D. J. Mitchell and B. W. Ninham, *J. Chem. Soc., Faraday Trans. 2*, 1976, **72**, 1525.
49 J. C. Eriksson and S. Ljunggren, *Langmuir*, 1990, **6**, 895.

Paper 9/03469B